Sensors & Diagnostics

PAPER

View Article Online
View Journal | View Issue

Cite this: *Sens. Diagn.*, 2023, **2**, 893

Synthesis of molybdenum nanoclusters from *Vitex negundo* leaves for sensing epinephrine in a pharmaceutical composition†

Harshita,[a] Sanjay Jha,[b] Tae-Jung Park [c] and Suresh Kumar Kailasa *[a]

Received 21st March 2023,
Accepted 29th May 2023

DOI: 10.1039/d3sd00063j

rsc.li/sensors

The fabrication of metal nanoclusters (NCs) obtained from medicinal plant extracts for the detection of biomolecules has attracted a lot of interest recently. In this work, green chemistry is used to synthesize cyan fluorescent molybdenum nanoclusters (MoNCs) for the selective detection of epinephrine. The MoNCs were synthesized by using $MoCl_5$ as a metal precursor and *Vitex negundo* (*V. negundo*) plant extract as a capping agent. With the addition of epinephrine, the intensity of the emission peak of *V. negundo*-MoNCs at 495 nm was drastically quenched (68%) on the basis of the inner filter effect (IFE) between *V. negundo*-MoNCs and epinephrine demonstrating that *V. negundo*-MoNCs can be used as sensing probe for the epinephrine detection. Further, the effect of pH on the fluorescence response of *V. negundo*-MoNCs was investigated for sensing epinephrine. Moreover, the *V. negundo*-MoNCs fluorescent probe exhibited a good linear range of (0.25–10 μM) for epinephrine with a detection limit of 0.46 μM. The MTT assay was used to investigate the cytotoxicity of *V. negundo*-MoNCs on the A549 lung cancer cell line, demonstrating the biocompatibility of MoNCs. This approach was further successfully employed for quantifying epinephrine in pharmaceutical samples.

1. Introduction

Neurotransmitters, also known as the chemical messengers of the body, are the chemical molecules, which are responsible for transmitting messages as signals through neurons to the target cell.[1] The adrenal gland secretes epinephrine, a crucial catecholamine neurotransmitter in the nervous system.[2] By speeding up the heart rate, it can increase the chance that cardiac arrest patients will survive.[3] In response to a violent event, intense emotions like fear, rage, or any other form of excitement trigger the secretion of epinephrine into the blood, which raises the heart rate, sugar metabolism, blood pressure, and muscle contractions. The body prepares for vigorous activity as a result of this reaction, known as the "flight or fight reaction".[4] Early-stage diagnosis is crucial since the usual level of epinephrine in the human body is 764.3 pM, and abnormalities in this level can cause detrimental disorders such Parkinson's disease, multiple sclerosis, hypertension and Alzheimer's disease.[5]

Nanomaterials, for example, carbon nanomaterials, metal nanoparticles, metal oxide nanomaterials, polymers, biomaterials and nanohybrids,[6,7] have gained prominence as effective investigative probes due to their outstanding physicochemical properties, high surface-to-volume ratios, high adsorption, and reactive capacities. It is challenging to achieve these characteristics while utilising conventional material.[8] Various kinds of nanomaterials (0D–3D) have been utilized to enhance the sensor selectivity, sensitivity and limit of detection amongst various metrics. With the incorporation of these nanostructures into electrochemical,[9,10] optical spectroscopy, high-performance liquid chromatography (HPLC) and gas/liquid chromatography-mass spectrometry (GC-MS) techniques, the analytical features of these techniques are greatly improved.[11] For instance, in a report rGO nanosheets were decorated with Pd NPs by utilizing microwave-assisted *in situ* reduction and exfoliation methods in order to examine their hydrogen detection ability under various conditions. The detection capability further was evaluated at different hydrogen concentrations (up to 1%), temperatures, and relative humidities (up to ~44%).[12] An organoclay/polypyrrole-alginate (OC/Ppy-A) nanocomposite-modified glassy carbon sensor (MGCS) was developed for sensitive detection of greenhouse gas (CO_2) in seawater and brackish samples and examined using electrochemical

[a] *Department of Chemistry, Sardar Vallabhbhai National Institute of Technology, Surat-395007, India. E-mail: sureshkumarchem@gmail.com, skk@chem.svnit.ac.in*
[b] *ASPEE Shakilam Biotechnology Institute, Navsari Agricultural University, Surat 39500, Gujarat, India*
[c] *Department of Chemistry, Research Institute of Chem-Bio Diagnostic Technology, Chung-Ang University, 84 Heukseok-ro, Dongjak-gu, Seoul 06974, Republic of Korea*
† Electronic supplementary information (ESI) available. See DOI: https://doi.org/10.1039/d3sd00063j

impedance spectroscopy and cyclic voltammetry (CV).[13] Compared to the bare glassy carbon sensor (GCS), the fabricated MGCS demonstrated a superior five-fold CV signal for detection of CO_2. Various techniques for the quantification of epinephrine using nanomaterials have been described in the literature such as electrochemistry,[14,15] colorimetric,[16] chemiluminescence,[17] surface-enhanced Raman spectroscopy,[18] HPLC,[19] and capillary electrophoresis.[20] However, the majority of these techniques are not capable of quick on-site detection, mainly in remote areas, because of their laborious operation and high cost. In this aspect, a fluorescence technique for detection is very appealing as it is simple and requires a low cost of operation. A fluorescent biosensor is advantageous because of its characteristics such as selectivity, simplicity, sensitivity, minimal cost instrument, fastness and visual identification.[21–23] Furthermore, the use of nanomaterials as probes has significantly improved the effectiveness of numerous analytical approaches for the identification of epinephrine in several clinical biological fluids. For example, an ordered mesoporous carbon/nickel oxide nanocomposite was used as a substrate for the sensing of epinephrine with a limit of detection (LOD) of 8.5×10^{-8} M.[14] Further, 3D-laccase–$Cu_3(PO_4)_2{\cdot}3H_2O$ microflowers were fabricated for the colorimetric detection of epinephrine.[24] Similarly, a molecularly imprinted polymer was decorated on the surface of an MXene/carbon nanohorn for the voltammetric determination of epinephrine.[25] Although the above analytical techniques exhibited good selectivity and impressive sensitivity, they required tedious synthetic routes and specific ligands. Hence, one of the most important ways to counteract the negative effects of producing nanomaterials chemically is through green synthesis.[26] As a result, biosynthesis of nanomaterials using plants emerged as a secure, affordable, and more environmentally friendly substitute.[27] The majority of the workers are interested in using plant extracts to synthesize nanomaterials because they contain a variety of phytoactive compounds that serve as stabilizing and reducing agents simultaneously, resulting in a simpler, quicker, and more affordable method.[26] Fluorescent metal NCs have developed into promising fluorescent nanostructures due to their distinct physicochemical and optical properties, flexibility of surface modification, nontoxicity, size-dependent luminescence abilities, excellent photostability, and water dispersity.[28,29] Because of their distinctive optical, electrical, and physical attributes, metal NCs have been successfully used for sensing, bioimaging, and catalysis applications.[30] They have also been successfully used to detect a wide range of analytes, including biomarkers, drugs, biomolecules, and nucleic acids.[31–34] Nowadays, MoNCs which are not been explored much yet have become a fascinating topic in nanoscience and analytical chemistry research.[35,36] For example, 6-aza-2-thiothymine (ATT) capped MoNCs have been fabricated to recognize cancer drug methotrexate with a LOD of 1.28 nM.[37] Similarly, another MoNCs using thiolated dithiothreitol (DTT) as capping agents were fabricated and used as bioimaging probes for imaging HaCaT, A549, and RPTEC cells owing to their smaller size and high biocompatibility.[38]

As far as we know, there are not many studies in the literature that utilize plant extracts for the green synthesis of fluorescent molybdenum NCs. The novelty of the method is the nontoxic approach for plant-based synthesis of MoNCs. The production proved to be easy and eco-friendly with natural reagents and less harsh chemicals as compared to chemically synthesized MoNCs. In addition, the presence of an array of phytochemicals in the *V. negundo* plant extract acts as natural reducing and stabilizing agents for MoNCs production. Therefore, we report herein the green synthesis of cyan colored fluorescent MoNCs as sensing probe for the detection of epinephrine by using *V. negundo* plant extract as a stabilizing agent. The as-fabricated *V. negundo*-MoNCs displayed a quantum yield (QY) of 24.04%. The synthesized *V. negundo*-MoNCs have good stability and specific selectivity towards the neurotransmitter biomarker epinephrine (Scheme 1). The as-synthesized *V. negundo*-MoNCs have the potential to sense epinephrine in its pharmaceutical samples, revealing the practical utility of probe in pharmaceutical industries.

2. Experimental

2.1. Chemicals and materials

Epinephrine used in this work was obtained from Sigma Aldrich. *Vitex negundo* leaves were bought from Navsari Agriculture University, Surat, Gujarat, India. $MoCl_5$ was purchased from TCI Chemicals. The other biomarkers were bought from Sigma Aldrich, USA. The water utilized for the entire research was purified using a Milli-Q water purifying system. The solvents and chemicals utilized throughout the full analysis were of analytical standard.

2.2. Instrumentation

A Cary Eclipse fluorescence spectrometer from Agilent Technologies and a Maya Pro 2000 spectrophotometer (Ocean Optics, USA) were used to accomplish fluorescence and absorption spectral investigations. An alpha II Fourier-transform infrared (FT-IR) spectrometer from Bruker, Germany was employed to measure the FT-IR spectra. The morphology of *V. negundo*-MoNCs was revealed through high-resolution transmission electron microscopy (HR-TEM) (JEM 2100, JEOL Japan).

2.3. Extraction of phytochemicals from the *V. negundo* leaf extract

The green leaves of *V. negundo* were taken, cleaned, washed with tap water, and afterwards rinsed using deionized water to extract the phytochemicals. Further, crushing of the leaves was done followed by drying for 24 h. Later, 50 mg of green leaves were taken in 10 mL of distilled water

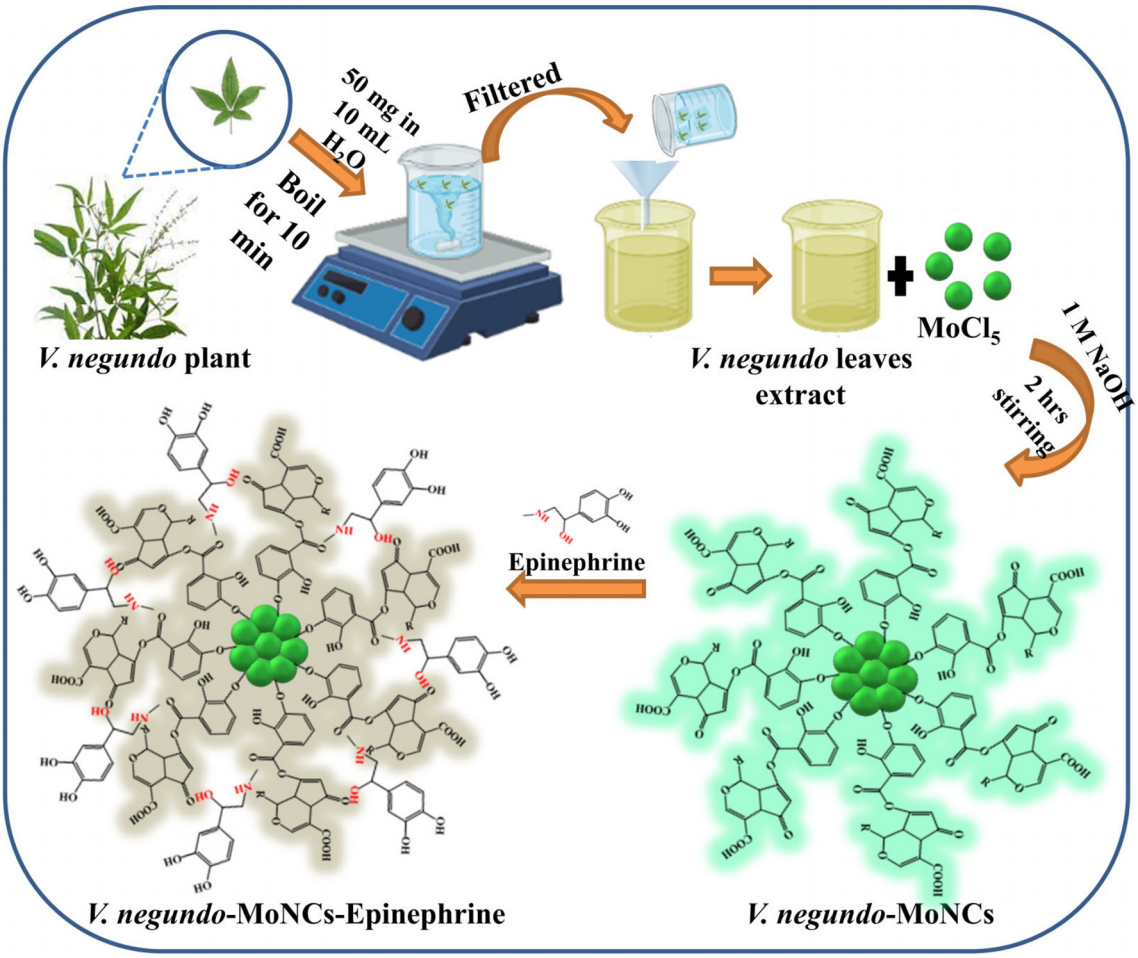

Scheme 1 Schematic illustration of phytochemical extraction from *V. negundo* leaves for the synthesis of cyan colored fluorescent *V. negundo*-MoNCs for sensing epinephrine.

which was then heated to boil for 10 till the solution was reduced to half of 10 mL. The leaf extract was obtained by filtering the supernatant through Whatman paper and was then kept at 4 °C for later use. The obtained extract served as a stabilizing and reducing agent for the synthesis of MoNCs.

2.4. Preparation of *V. negundo*-MoNCs

The biosynthesis of cyan colored fluorescent MoNCs (*V. negundo*-MoNCs) was accomplished using $MoCl_5$ as a precursor and *V. negundo* extract as a ligand. Briefly, 3 mL of the leaf extract was added into 7 mL (10 mM) of $MoCl_5$ and stirred for 2 min. The solution pH was adjusted using 1.0 mL of NaOH (1 M), and the resulting orange colored mixture solution was stirred for 2 h at room temperature to obtain a pale yellowish solution which confirms the formation of *V. negundo*-MoNCs. The final green-synthesized MoNCs were refrigerated at 4 °C until further usage. The as synthesized *V. negundo*-MoNCs displayed cyan colored fluorescence at 365 nm in UV light, which further verified the synthesis of *V. negundo*-MoNCs.

2.5. Fluorescence detection of epinephrine using *V. negundo*-MoNCs as probe

In a typical experiment for epinephrine detection, 1000 μL of *V. negundo*-MoNCs solution was added separately containing 500 μL of various biomarkers, namely myoglobin, normetanephrine, uric acid, cortisone, cortisol, dipicolinic acid, sodium selenite, methyl selenocysteine, and epinephrine, and the solution was vortexed for 60 s and left to stand for about 5 min. Furthermore, the fluorescence spectra of the above solutions were taken at 430 nm, and the change in their emission intensity was observed. An incredible change was obtained with 68% quenching in the fluorescence intensity of *V. negundo*-MoNCs for biomarker epinephrine. This illustrates that synthesized *V. negundo*-MoNCs behave as a sensor for the detection of epinephrine.

3. Results and discussion

3.1. Characterization and synthesis of *V. negundo*-MoNCs

The *V. negundo* extract contains a variety of phytochemical constituents including resveratrol, phenol, taraxerol, tannin, vitamin, carotene, flavonoids, phytosterols, keto-steroids

and indanes, providing good architecture for the fabrication of metal NCs. These characteristics make the *V. negundo* a suitable ligand for encapsulating MoNCs. The cyan colored fluorescent MoNCs were generated in a single step reaction using a solution containing the *V. negundo* extract and $MoCl_5$ as precursors in the presence of NaOH solution. A range of concentrations (1, 5, 10 and 20 mM) of $MoCl_5$ were investigated so as to identify the optimal concentration of $MoCl_5$ for the fabrication of cyan color MoNCs from the *V. negundo* leaf extract. It was observed that the emission spectra at 495 nm were obtained with good intensity only after using 10 mM of $MoCl_5$, suggesting the development of fluorescent MoNCs (Fig. S1a†). In a similar way, separate volumes from 1 mL to 5 mL of the *V. negundo* leaf extract have been explored for the synthesis of fluorescent MoNCs with an active phytochemical architecture. It was observed that using 3 mL of *V. negundo* solution and 7 mL of 10 mM $MoCl_5$ resulted in generating a good emission spectrum of *V. negundo*-MoNCs (Fig. S1b†). Moreover, the time of reaction is a crucial factor in the development of NCs. To determine the optimal time of reaction, the emission spectrum of *V. negundo*-MoNCs was studied at various time intervals, and the optimum results were obtained from a reaction time of 150 min (Fig. S2†); after 150 min the fluorescence intensity of the *V. negundo*-MoNCs starts decreasing, indicating that 150 min is the optimal time for the generation of *V. negundo*-MoNCs. These results indicate that 7 mL of 10 mM $MoCl_5$, 3 mL of the *V. negundo* extract, 1 mL of 1 M NaOH and 150 min as the time of reaction are the best parameters for the formation of *V. negundo*-MoNCs.

The synthesized *V. negundo*-MoNCs were analyzed by fluorescence and UV-visible spectroscopy. The formed *V. negundo*-MoNCs have a pale yellow color solution in daylight and emit cyan color fluorescence when exposed to UV light at 365 nm. The absorbance peak maximum was observed at 319 nm. The *V. negundo*-MoNCs exhibited an emission peak maximum at 495 nm after exciting at 430 nm (Fig. 1). In order to determine the maximum emission intensity of *V. negundo*-MoNCs, the synthesized MoNCs were excited at various excitation wavelengths ranging from 370 nm to 450 nm, and the maximum emission intensity of *V. negundo*-MoNCs was observed at 495 nm upon exciting at 430 nm (Fig. S3†). The as-fabricated *V. negundo*-MoNCs are confirmed by the fluorescence and absorption spectrum spectral characteristics of $MoCl_5$, *V. negundo*, and *V. negundo*-MoNCs, which are displayed in Fig. S4.† These results demonstrate that the spectral features of *V. negundo*-MoNCs differ significantly in comparison to their spectral characteristics of precursors. The emission spectra of *V. negundo*-MoNCs at various time intervals were studied to determine the stability of *V. negundo*-MoNCs (Fig. S5†). These data demonstrated that *V. negundo*-MoNCs are stable for up to 120 days, which suggests that *V. negundo* effectively protected MoNCs, increasing the stability of MoNCs. The QY of *V. negundo*-MoNCs was determined to be 24.04% by taking quinine sulphate as a standard.

FT-IR analysis of the *V. negundo* extract and *V. negundo*-MoNCs was carried out to identify the surface functional groups of *V. negundo*-MoNCs (Fig. S6†). The peak at 3445 cm^{-1} represents the OH stretching of *V. negundo*; however, the OH stretching peak intensity increases in *V. negundo*-MoNCs. The peaks around 2925 and 2857 cm^{-1} indicate the C–H stretching in *V. negundo* and *V. negundo*-MoNCs. There is a significant increase in the peak intensities of *V. negundo*-MoNCs at 1632, 1453 and 1383 cm^{-1}, illustrating the carbonyl (–C═O) stretching, –CH stretching and OH bending. The FT-IR spectrum of *V. negundo*-MoNCs exhibits the sharp peaks at 1117 and 839 cm^{-1} corresponding to the –C–O stretching and C═C bending, whereas these peaks for *V. negundo* are not observed, confirming the binding and interaction of phytochemicals of *V. negundo* on the surface of the MoNCs.

The size and morphology of *V. negundo*-MoNCs were investigated by an HR-TEM technique. The HR-TEM images of the *V. negundo*-MoNCs are shown in Fig. 2a–d, revealing a clear depiction of the fabrication of small spherical shaped *V. negundo*-MoNCs with uniform size distribution of 2.39 ± 0.64 nm (Fig. 2d). The time of decay for *V. negundo*-MoNCs was examined by the fluorescence lifetime study and observed that *V. negundo*-MoNCs displayed a lifetime of 3.02 ns (Fig. S7†). The X-ray diffraction (XRD) data reveal the formation of the crystalline structure of *V. negundo*-MoNCs (Fig. S8†). The sharp diffraction peaks (2θ) at 19.98°, 24.48°, 27.24°, 31.46°, 32.14°, 39.74°, and 49.40° representing the lattice planes (200), (110), (021), (130), (111), (060) and (002) confirm the crystalline structure of *V. negundo*-MoNCs.[39–42]

The elemental composition and oxidation states of *V. negundo*-MoNCs were explored by X-ray photoelectron spectroscopy (XPS). The presence of Mo, C, N, S and O in the obtained *V. negundo*-MoNCs was verified by the survey spectra of XPS (Fig. S9a†). Using the suitable fitting results, Fig. S9b† displays the Mo 3d core level XPS spectra. The Mo 3d spectrum deconvoluted into two peaks at 231.9 eV

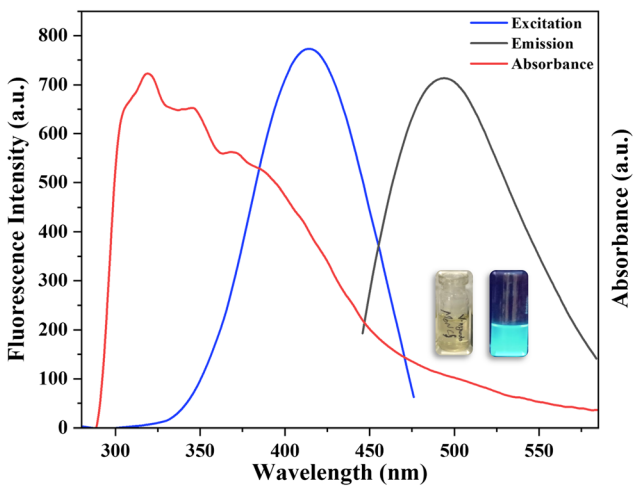

Fig. 1 Optical (emission/excitation) and absorbance spectral characteristics of *V. negundo*-MoNCs.

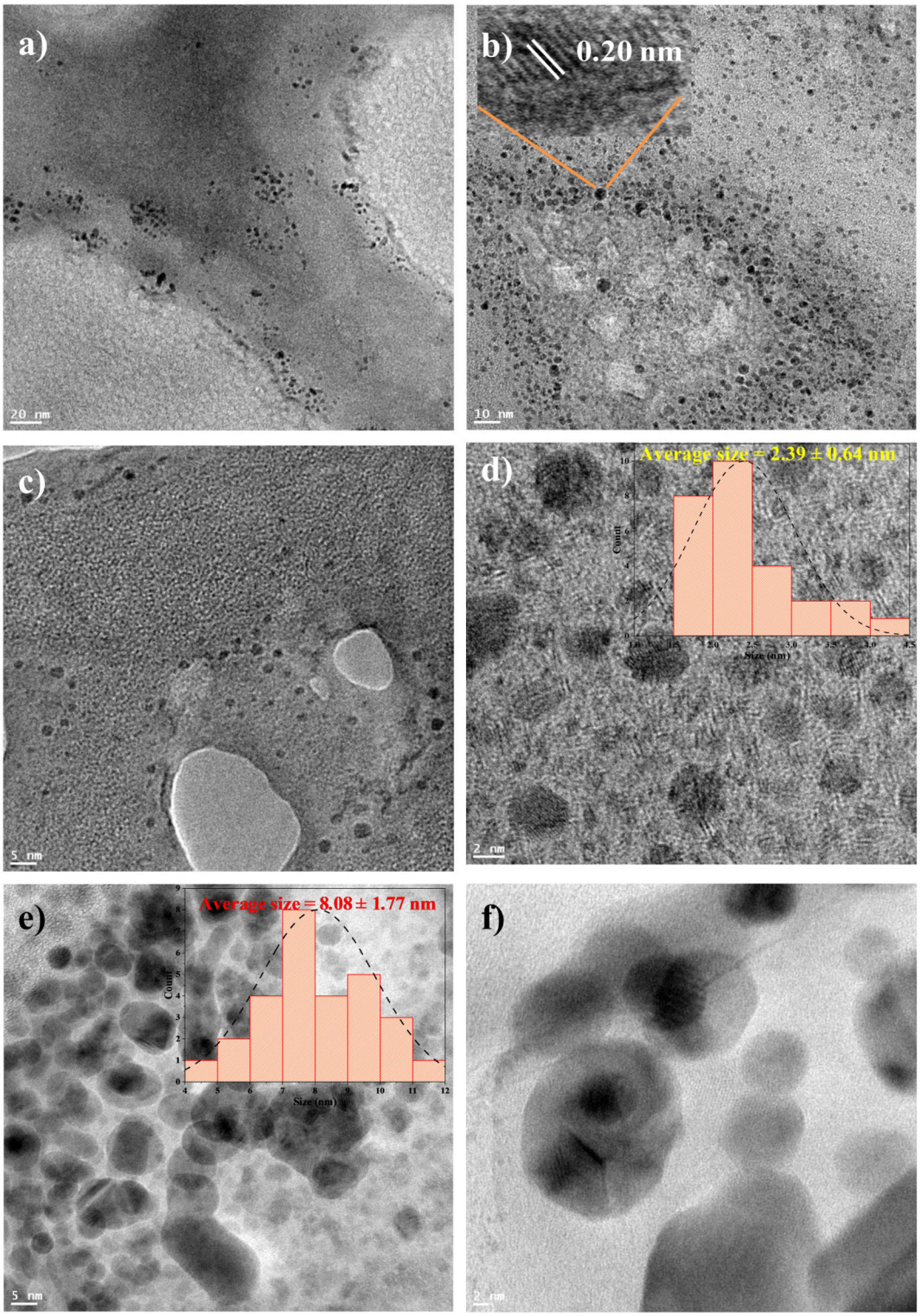

Fig. 2 HR-TEM of V. negundo-MoNCs at (a) 20 nm, (b) 10 nm with the depiction of distance between lattice fringes (c) 5 nm, and (d) 2 nm scale bars and inset: histogram representing the average size of *V. negundo*-MoNCs. (e) HR-TEM images of the *V. negundo*-MoNCs–epinephrine complex at 5 nm. Inset: Histogram representing the average size of *V. negundo*-MoNCs–epinephrine complex. (f) HR-TEM image of the *V. negundo*-MoNCs–epinephrine complex at 2 nm scale bar.

and 234.9 eV signifies the oxidation state of Mo^{3+} and Mo^{5+} $3d_{3/2}$ in the *V. negundo*-MoNCs.[43,44] The results indicates the presence of distinctive peaks for Mo^{3+} and Mo^{5+} in *V. negundo*-MoNCs with the dominance peak for Mo is the 3+ oxidation state, confirming the formation of *V. negundo*-MoNCs.

3.2. Recognition ability of *V. negundo*-MoNCs towards epinephrine

The molecular recognition ability of *V. negundo*-MoNCs was determined by the fluorescence spectra at 495 nm after adding a series of biomarkers (myoglobin, normetanephrine, uric acid, cortisone, cortisol, dipicolinic acid, sodium selenite, methyl selenocysteine, and epinephrine, 500 μM). Fig. 3a shows that the fluorescence intensity of *V. negundo*-MoNCs was quenched by 68% after the addition of epinephrine, whereas other biomarkers had no noticeable impact on the emission spectrum of *V. negundo*-MoNCs. This indicates that *V. negundo*-MoNCs exhibit high selectivity for epinephrine. Moreover, the cyan fluorescence of *V. negundo*-MoNCs was quenched after adding epinephrine, which was visible to the naked eye as shown in Fig. 3b. These results confirmed that *V. negundo*-MoNCs serve as a biosensor for the recognition of epinephrine by a "fluorescence turn-off" mechanism.

3.3. pH study

To determine the impact of pH on the fluorescence response of *V. negundo*-MoNCs, the emission spectrum of the as-synthesized *V. negundo*-MoNCs with or without epinephrine was examined at a broad range of phosphate-buffered saline (PBS) pH values ranging from 2.0 to 12.0. As shown in Fig. S10a,† there is a decrement in the fluorescence intensity at pH 2 or 3 and a further rise in pH from 4 to 12 leads to an increase in intensity of the emission spectra, indicating the pH dependent response of *V. negundo*-MoNCs. Under highly acidic environment, the surface active carboxylic acid group of *V. negundo*-MoNCs is bonded to H^+ ions, resulting in the generation of [*V. negundo*-MoNCs–H]$^+$. It induces MoNCs to aggregate, which reduces the intensity of the fluorescence. In contrast, in an alkaline environment, the COOH group on the surface of *V. negundo*-MoNCs deprotonate into carboxylate, thereby increasing the fluorescence intensity. Similarly, when epinephrine was introduced into *V. negundo*-MoNCs at PBS pH ranging from 2.0 to 12.0 (Fig. S10b†), the *V. negundo*-MoNC emission spectra intensity was quenched in every pH. However, at pH 2 or 3 a further decrement in the fluorescence intensity was due to the aggregation of NCs as explained above. Thus, *V. negundo*-MoNCs function as a fluorescent sensor for quantifying epinephrine without optimization of buffer pH.

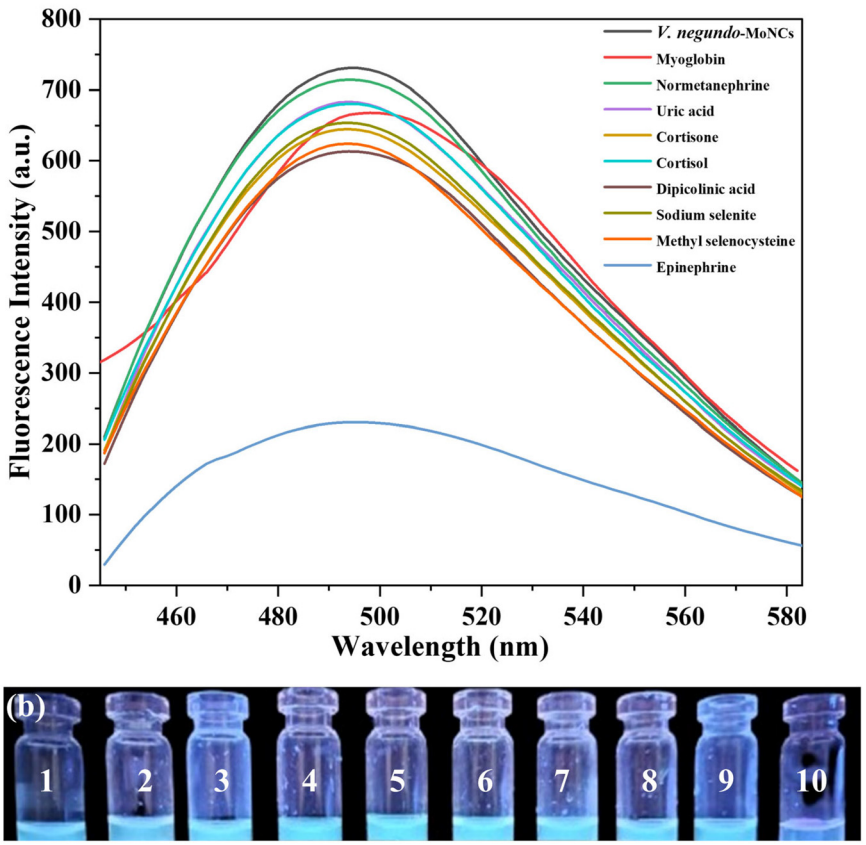

Fig. 3 (a) Emission spectrum of *V. negundo*-MoNCs with numerous biomarkers (myoglobin, normetanephrine, uric acid, cortisone, cortisol, dipicolinic acid, sodium selenite, methyl selenocysteine, and epinephrine, 500 μM). (b) Photograph depicting changes in the fluorescence intensity of *V. negundo*-MoNCs after adding various biomarkers (1) *V. negundo*-MoNCs, (2) myoglobin, (3) normetanephrine, (4) uric acid, (5) cortisone, (6) cortisol, (7) dipicolinic acid, (8) sodium selenite, (9) methyl selenocysteine, and (10) epinephrine under UV light of 365 nm.

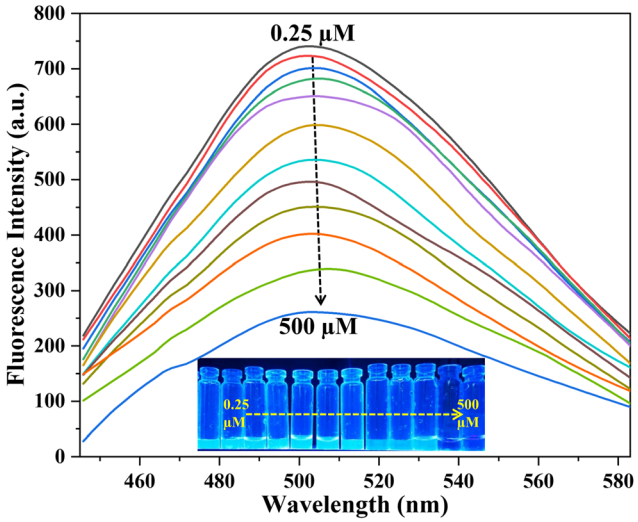

Fig. 4 Fluorescence emission spectral changes of *V. negundo*-MoNCs in the presence of various concentrations of epinephrine (0.25–500 μM). Inset: Fluorescence variations in *V. negundo*-MoNCs as the concentration of epinephrine increases from 0.25 to 500 μM in UV at 365 nm.

3.4. Sensitivity of *V. negundo*-MoNCs towards epinephrine

The sensitivity study of *V. negundo*-MoNCs after adding aliquots of epinephrine (0.25–500 μM) was performed as shown in Fig. 4. It was noticed that the emission spectra at 495 nm displayed a significant decline in intensity with an increasing concentration of epinephrine (0.25–500 μM). This demonstrates that *V. negundo*-MoNCs fluorescence response, which can be seen in Fig. S11,† is highly sensitive to epinephrine at 495 nm and is in linear relationship with the epinephrine concentration in the range of (0.25–10 μM). Using this, a linear equation and coefficient of correlation R^2 (y = 0.035x + 1.049, R^2 = 0.993 for epinephrine) were obtained between the fluorescence intensity ratio and concentration of epinephrine (Fig. S11†) for the detection of epinephrine (the ratio I_0/I; here I_0 refers to the intensity of *V. negundo*-MoNCs without epinephrine and I represents the intensity of *V. negundo*-MoNCs with epinephrine). The LOD is 0.46 μM, obtained by using the 3σ rule, wherein σ refers to the standard deviation for blank *V. negundo*-MoNCs. Comparison of the current method with the previously reported techniques for epinephrine detection is shown in Table 1, revealing that *V. negundo*-MoNCs acted as a promising fluorescent probe for the detection of epinephrine.

3.5. Sensing mechanism

To examine the mechanism for sensing of epinephrine using *V. negundo*-MoNCs as a fluorescent sensor, the fluorescence and UV-visible spectrum, HR-TEM, dynamic light scattering (DLS), fluorescence lifetime and zeta potential of *V. negundo*-MoNCs were investigated with or without epinephrine. The reason for the fluorescence quenching of *V. negundo*-MoNCs after addition of epinephrine might represent the IFE which takes place between the donor (*V. negundo*-MoNCs) and acceptor (epinephrine). The excitation spectra of *V. negundo*-MoNCs overlap with the epinephrine absorbance spectrum (Fig. S12a†), suggesting the quenching in the emission intensity of *V. negundo*-MoNCs by epinephrine *via* the IFE. The UV-visible spectra of *V. negundo*-MoNCs–epinephrine as shown in (Fig. S12b†) shifted to a longer wavelength with a sharp peak at 343 nm as compared to *V. negundo*-MoNCs, indicating the interaction of epinephrine with *V. negundo*-MoNCs. The HR-TEM image confirmed the aggregation of the *V. negundo*-MoNCs after adding epinephrine. It was found that the average size of the *V. negundo*-MoNCs increases to 8.08 ± 1.77 nm as depicted in the HR-TEM image (Fig. 2e and f). This is also confirmed by the DLS data since aggregation causes the hydrodynamic diameter of the *V. negundo*-MoNCs to rise from 4.86 ± 1.44 nm to 18.12 ± 8.16 nm on addition of epinephrine (Fig. S13†). The zeta potential of epinephrine observed was −1.3 mV (Fig. S14a†), and the zeta potential of *V. negundo*-MoNCs significantly decreased from −16.9 mV to −8.9 mV (Fig. S14b and c†) after adding epinephrine, demonstrating the electrostatic interaction between *V. negundo*-MoNCs and epinephrine. The decline in the average lifetime of *V.*

Table 1 Comparison of the *V. negundo*-MoNCs-based fluorescence method with the previously reported techniques for epinephrine detection

Method	Material	Linear range (μM)	LOD (μM)	Ref.
Fluorescent sensor	MoS_2 quantum dots	0.2–40	0.05	45
Chemically modulated fluorescent sensor	—	0.05–10	0.5	46
Colorimetric sensor	Laccase-mineral hybrid microflowers	1–400	0.6	47
Electrochemical sensor	Multi-walled carbon nanotube modified glassy carbon electrode	50–1150	7.20	48
Electrochemical sensor	*o*-Phenylenediamine–epinephrine-molecularly imprinted polymer	0–100	Less than 13	49
Electrochemical sensor	Nickel oxide-reduced graphene oxide	50–1000	10	50
Electrochemical sensor	Carbon quantum dots/copper oxide nanocomposite	10–100	15.99	51
Fluorescent sensor	*V. negundo*-MoNCs	0.25–10	0.46	Present method

negundo-MoNCs from 3.02 ns to 1.65 ns in *V. negundo*-MoNCs–epinephrine suggests the identification of epinephrine by dynamic quenching (Fig. S7†).

The FT-IR spectrum of *V. negundo*-MoNCs and *V. negundo*-MoNCs after the addition of epinephrine were examined to ascertain the interaction of epinephrine with the *V. negundo*-MoNCs (Fig. S15†). The FT-IR results demonstrated the increase in the distinctive peaks of –OH, –C–H, C═O and C═C bending in *V. negundo*-MoNCs by the introduction of epinephrine; however a significant increment in peak intensity at 1381 cm^{-1} representing –C–N stretching was observed in *V. negundo*-MoNCs–epinephrine leading to significant interaction between epinephrine and *V. negundo*-MoNCs. The sharp –C–O stretching peak at 1117 cm^{-1} was diminished in the FT-IR spectra of *V. negundo*-MoNCs–epinephrine, resulting in a broad peak, indicating the formation of *V. negundo*-MoNC–epinephrine complex.

3.6. Selectivity of *V. negundo*-MoNCs towards epinephrine

The selective nature of *V. negundo*-MoNCs towards epinephrine was investigated with some interferents like cations (Na^+, Cd^{2+}, Cu^{2+}, Zn^{2+}, Fe^{3+}, Co^{2+}, and Cr^{6+}, 500 μM), anions (Br^-, Cl^-, I^-, SO_4^{2-}, and PO_4^{3-}, 500 μM) and biomarkers (dopamine, phenylalanine, tyrosine, and normetanephrine, 500 μM). As depicted in Fig. S16,† the fluorescence intensity of *V. negundo*-MoNCs remain unaffected after introducing the above-mentioned interfering agents. Furthermore, the emission intensity of *V. negundo*-MoNCs was markedly reduced only after the introduction of epinephrine to the interferents, demonstrating the selective detection ability of *V. negundo*-MoNCs toward epinephrine.

3.7. Assessment of cytotoxicity of *V. negundo*-MoNCs

The cytotoxic effect of *V. negundo*-MoNCs was evaluated on the A549 lung carcinoma cell line using the methyl thiazolyl tetrazolium (MTT) method (Fig. 5). A549 lung cancer cells were incubated with various concentrations of *V. negundo*-MoNCs (15.25–125 μg mL^{-1}). The viabilities of cell are 93.33%, 86.52%, 81.97%, and 71.44% by using 15.25, 31.25, 62.5, and 125 μg mL^{-1} *V. negundo*-MoNCs, demonstrating the biocompatibility and nontoxicity of *V. negundo*-MoNCs and their potential utility as a biosensor for the visualization of different cells.

3.8. Analysis of epinephrine in its pharmaceutical composition

The proposed method was evaluated by quantifying epinephrine in a pharmaceutical composition. For this, adrenaline injection of Rathi Laboratories (Hindustan) Pvt. Ltd. containing 1 mg of epinephrine was procured from a local medical store in Surat, India. As epinephrine was present in the adrenaline injection at a concentration of 1 mg mL^{-1}, different concentrations of 100, 250 and 500 μM of epinephrine were made, and by employing *V. negundo*-MoNCs based sensor, epinephrine was quantified. As provided in Table S1 of the ESI,† epinephrine recovery values were in between 98.54 to 99.41% with a relative standard deviation (RSD) of <2%, displaying the probe usability and viability for epinephrine quantification in pharmaceutical samples.

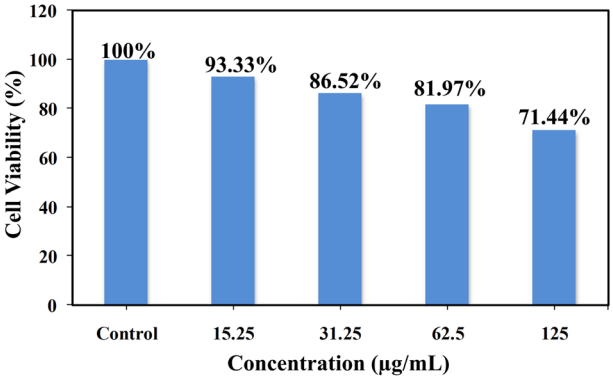

Fig. 5 Cytotoxicity study of *V. negundo*-MoNCs on the A549 lung carcinoma cell line by an MTT assay.

4. Conclusions

A novel and simple method is developed for the synthesis of MoNCs by using *V. negundo* leaf extract as a stabilizing and reducing agent. The as-synthesized *V. negundo* capped MoNCs exhibits cyan color fluorescence under UV light with a QY of 24.04%. The *V. negundo*-MoNCs emission intensity was drastically quenched on adding epinephrine, offering the possibility to detect the analyte by a "turn-off" mechanism. The technique provides a rapid response, inexpensive miniaturized analytical strategy for the specific quantification of epinephrine. The method enables a sensitive fluorescence determination of epinephrine with a LOD of 0.46 μM. The biosensor was satisfactorily used to detect epinephrine in a pharmaceutical composition. Hence, the as-fabricated *V. negundo*-MoNCs can be used as a miniaturized sustainable analytical tool for the identification of epinephrine in real samples.

Conflicts of interest

There are no conflicts to declare.

Acknowledgements

Authors greatly acknowledge the Department of Science and Technology (DST), Government of India (EMR/2016/002621/IPC) for providing a research grant for this work.

References

1 M. M. Charithra, J. G. Manjunatha, A. A. Al-Kahtani, A. M. Tighezza and N. Ataollahi, *Top. Catal.*, 2022, 1–11.

2 C. Wang, Q. Han, P. Liu, G. Zhang, L. Song, X. Zou and Y. Fu, *ACS Sens.*, 2021, **6**, 252–258.
3 Q. Huang, Y. Liu, C. Zhang, Z. Zhang, F. Liu and J. Peng, *ACS Omega*, 2020, **5**, 8423–8431.
4 B. Soleymani, B. Zargar and S. Rastegarzadeh, *J. Iran. Chem. Soc.*, 2020, **17**, 1013–1025.
5 T. M. Thenrajan, S. Ramasamy, P. K. Chidambaram and J. Wilson, *Mater. Chem. Phys.*, 2022, **276**, 125366.
6 T. Kant, N. S. Dahariya, V. K. Jain, B. Ambade and K. Shrivas, *Silver Nanomaterials for Agri-Food Applications*, Elsevier, 2021, pp. 429–452.
7 R. Kumar, W. Dias, R. J. Rubira, A. V. Alaferdov, A. R. Vaz, R. K. Singh, S. R. Teixeira, C. J. Constantino and S. A. Moshkalev, *IEEE Trans. Electron Devices*, 2018, **65**, 3943–3949.
8 A. Thakur and A. Kumar, *Sci. Total Environ.*, 2022, **834**, 155219.
9 D. S. Rana, S. Kalia, R. Kumar, N. Thakur, R. K. Singh and D. Singh, *Environ. Nanotechnol., Monit. Manage.*, 2022, **18**, 100724.
10 D. S. Rana, S. Kalia, R. Kumar, N. Thakur, D. Singh and R. K. Singh, *Mater. Chem. Phys.*, 2022, **287**, 126283.
11 E. C. Welch, J. M. Powell, T. B. Clevinger, A. E. Fairman and A. Shukla, *Adv. Funct. Mater.*, 2021, **31**, 2104126.
12 H. Hashtroudi, R. Kumar, R. Savu, S. Moshkalev, G. Kawamura, A. Matsuda and M. Shafiei, *Int. J. Hydrogen Energy*, 2021, **46**, 7653–7665.
13 M. Elfiky, R. Kumar and A. Beltagi, *J. Electroanal. Chem.*, 2022, **926**, 116926.
14 X. Yang, P. Zhao, Z. Xie, M. Ni, C. Wang, P. Yang, Y. Xie and J. Fei, *Talanta*, 2021, **233**, 122545.
15 S. Kalia, D. S. Rana, N. Thakur, D. Singh, R. Kumar and R. K. Singh, *Mater. Chem. Phys.*, 2022, **287**, 126274.
16 M. Ying, G. Yang, Y. Xu, H. Ye, X. Lin, Y. Lu, H. Pan, Y. Bai and M. Du, *Analyst*, 2022, **147**, 40–47.
17 M. Amjadi, T. Hallaj, J. L. Manzoori and T. Shahbazsaghir, *Spectrochim. Acta, Part A*, 2018, **201**, 223–228.
18 B. Zhou, X. Li, X. Tang, P. Li, L. Yang and J. Liu, *ACS Appl. Mater. Interfaces*, 2017, **9**, 7772–7779.
19 D. Wu, H. Xie, H. Lu, W. Li and Q. Zhang, *Biomed. Chromatogr.*, 2016, **30**, 1458–1466.
20 A. Roychoudhury, K. A. Francis, J. Patel, S. K. Jha and S. Basu, *RSC Adv.*, 2020, **10**, 25487–25495.
21 H. Singh, A. Bamrah, S. K. Bhardwaj, A. Deep, M. Khatri, K. H. Kim and N. Bhardwaj, *J. Hazard. Mater.*, 2021, **407**, 124379.
22 S. K. Pradhan, B. Ambade and P. K. Tarafder, *Appl. Radiat. Isot.*, 2020, **160**, 109126.
23 S. K. Pradhan and B. Ambade, *Radiochim. Acta*, 2021, **109**, 195–203.
24 M. Zhang, Y. Zhang, C. Yang, C. Ma, Y. Zhang and J. Tang, *Microchem. J.*, 2022, **172**, 106911.
25 S. Chen, M. Shi, J. Yang, Y. Yu, Q. Xu, J. Xu, X. Duan, Y. Gao and L. Lu, *Microchim. Acta*, 2021, **188**, 1–11.
26 A. M. Abdelfatah, M. Fawzy, A. S. Eltaweil and M. E. El-Khouly, *ACS Omega*, 2021, **6**, 25397–25411.
27 M. Hosny, A. S. Eltaweil, M. Mostafa, Y. A. El-Badry, E. E. Hussein, A. M. Omer and M. Fawzy, *ACS Omega*, 2022, **7**, 3121–3133.
28 B. Wang, M. Zhao, M. Mehdi, G. Wang, P. Gao and K. Q. Zhang, *Mater. Chem. Front.*, 2019, **3**, 1722–1735.
29 J. Yang, Y. Peng, S. Li, J. Mu, Z. Huang, J. Ma, Z. Shi and Q. Jia, *Coord. Chem. Rev.*, 2022, **456**, 214391.
30 L. Farzin, M. Shamsipur, L. Samandari, S. Sadjadi and S. Sheibani, *Talanta*, 2020, **214**, 120886.
31 B. Li, P. Zhang, B. Zhou, S. Xie, A. Xia, T. Suo, S. Feng and X. Zhang, *Anal. Chim. Acta*, 2021, **1148**, 238194.
32 Y. C. Chen, S. W. Hong, H. H. Wu, Y. L. Wang and Y. F. Chen, *Nanomaterials*, 2021, **11**, 1789.
33 S. Borse, Z. V. P. Murthy, T. J. Park and S. K. Kailasa, *ACS Appl. Nano Mater.*, 2021, **4**, 11949–11959.
34 X. Lin, L. Zou, W. Lan, C. Liang, Y. Yin, J. Liang, Y. Zhou and J. Wang, *Dalton Trans.*, 2022, **51**, 27–39.
35 M. R. Kateshiya, D. J. Joshi, M. A. Kumar, N. I. Malek and S. K. Kailasa, *J. Mol. Liq.*, 2022, **365**, 120139.
36 Y. Xu, R. Wang, J. Wang, J. Li, T. Jiao and Z. Liu, *J. Chem. Eng.*, 2021, **417**, 129233.
37 S. Borse, Z. V. P. Murthy and S. K. Kailasa, *J. Photochem. Photobiol., A*, 2023, **435**, 114323.
38 A. K. Sharma, S. Pandey, N. Sharma and H. F. Wu, *Mater. Sci. Eng., C*, 2019, **99**, 1–11.
39 S. K. Sen, S. Dutta, M. R. Khan, M. S. Manir, S. Dutta, A. Al Mortuza, S. Razia and M. A. Hakim, *Bionanoscience*, 2019, **9**, 873–882.
40 R. K. K. Reddy, S. Kailasa, B. G. Rani, N. Jayarambabu, H. Yasuhiko, G. V. Ramana and K. V. Rao, *SN Appl. Sci.*, 2019, **1**, 1–9.
41 S. Rajagopal, D. Nataraj, O. Y. Khyzhun, Y. Djaoued, J. Robichaud, K. Senthil and D. Mangalaraj, *CrystEngComm*, 2011, **13**, 2358–2368.
42 N. R. Dighore, P. L. Anandgaonker, S. T. Gaikwad and A. S. Rajbhoj, *Mater. Sci.-Pol.*, 2015, **33**, 163–168.
43 Y. Zhao, K. Kamiya, K. Hashimoto and S. Nakanishi, *J. Am. Chem. Soc.*, 2015, **137**, 110–113.
44 S. J. Xiao, X. J. Zhao, J. Zuo, H. Q. Huang and L. Zhang, *Anal. Chim. Acta*, 2016, **906**, 148–155.
45 F. Zhang, M. Wang, D. Zeng, H. Zhang, Y. Li and X. Su, *Anal. Chim. Acta*, 2019, **1089**, 123–130.
46 Y. Zhang, W. Ren, Y. Z. Fan, H. Q. Luo and N. B. Li, *Sens. Actuators, B*, 2020, **305**, 127463.
47 M. Zhang, Y. Zhang, C. Yang, C. Ma and J. Tang, *Talanta*, 2021, **224**, 121840.
48 L. V. da Silva, N. D. dos Santos, A. K. A. de Almeida, D. D. E. R. dos Santos, A. C. F. Santos, M. C. França, D. J. P. Lima, P. R. Lima and M. O. F. Goulart, *J. Electroanal. Chem.*, 2021, **881**, 114919.
49 B. Si and E. Song, *Microelectron. Eng.*, 2018, **187**, 58–65.
50 A. G. Ramu, A. Umar, A. A. Ibrahim, H. Algadi, Y. S. A. Ibrahim, Y. Wang, M. M. Hanafiah, P. Shanmugam and D. Choi, *Environ. Res.*, 2021, **200**, 111366.
51 S. E. Elugoke, O. E. Fayemi, A. S. Adekunle, P. S. Ganesh, S. Y. Kim and E. E. Ebenso, *J. Electroanal. Chem.*, 2023, **929**, 117120.